

Supporting Information: Fragment arrays for early druggability assessments

J. Aretz^{a,b}, Y. Kondoh^{c,d}, K. Honda^{c,d}, U. R. Anumala^e, M. Nazaré^e, N. Watanabe^{c,d,f}, H. Osada^{c,d} and C. Rademacher^{a,b}

^a Department of Biomolecular Systems, Max Planck Institute of Colloids and Interfaces, Potsdam, Germany.

^b Department of Biology, Chemistry, and Pharmacy, Freie Universität Berlin, Berlin, Germany.

^c Antibiotics Laboratory, RIKEN, Wako, Japan.

^d Chemical Biology Research Group, RIKEN Center for Sustainable Resource Science, Wako, Japan.

^e Leibniz Institut für Molekulare Pharmakologie (FMP), Berlin, Germany.

^f Industrial Biotechnology Research Laboratory, School of Biological Sciences, Universiti Sains Malaysia, Penang, Malaysia.

Table of content

| | |
|---|----|
| Materials and Methods | 2 |
| Supporting figures | 4 |
| Figure S1: Quality controls of the proteins used in this study. | 4 |
| Figure S2: Scan of an array with the highest gain to test for autofluorescence of the fragments. | 5 |
| Figure S3: Correlation of signal intensities of monomeric DC-SIGN carbohydrate recognition domain (CRD) with tetrameric DC-SIGN extracellular domain (ECD). | 6 |
| Figure S4: Recovery rates for hits from ¹⁹ F NMR screenings in array experiments using a PEG linker for fragment immobilization. | 6 |
| Figure S5: Correlation of the hit rate of the array screening with the ¹⁹ F NMR screening using a PEG linker for immobilization. | 7 |
| Chemoinformatic analysis | 8 |
| Figure S6: Difference between “non-hitters” and “regular-hitters” using MACCS fingerprints (Student’s <i>t</i> -test). | 8 |
| Additional discussion of chemoinformatic analysis | 12 |
| Figure S7: Principle component analysis of MACCS fingerprints of the fragment library and the “regular hitters” data set. | 13 |
| Figure S8: Known CA2 inhibitors and related fragments present on the chemical fragment array. | 14 |
| Figure S9: MNK inhibitors from fragment-based ligand design. | 15 |
| Figure S10: Chemical arrays using 0.2 μM protein in the presence of HEK293T cell lysate. | 15 |
| Notes and References | 16 |

Materials and Methods

Fragments used in this study

Fluorinated fragments and their selection were published earlier¹. Hits from a fragment-based NMR screening against murine Langerin will be published independently of this report (Aretz *et al.*, unpublished data). Quality controls were carried out for each compound using ¹H NMR (data not shown).

Protein preparation

DC-SIGN, murine and human Langerin as well as MNK were expressed as described elsewhere^{1,2}. Bovine Carbonic Anhydrase II (CA2) was purchased from Sigma-Aldrich (C3934, St. Louis, MO).

Protein quality controls

Purity and size of the proteins was assessed using sodium dodecyl sulfate polyacrylamide gel electrophoresis (SDS-PAGE) with subsequent Coumassie staining.

Fluorescent Labelling of C-type lectins

2 mL of protein solution was dialyzed overnight against 1 L of HBS buffer, pH 7.6, with 5 mM calcium chloride at 4°C. The protein solution was transferred into a 5 mL pear shaped flask and 30 mM mannose was added while stirring at room temperature. 1 mg Chromeo-642-NHS-ester dye (Active Motif, Carlsbad, CA) was dissolved in 10 µL DMF. From this stock solution, 1 µL was added to the protein solution in 0.2 µL steps. Afterwards, the reaction was carried out for 1 h at room temperature and then quenched with a final concentration of 50 mM ethanolamine, pH 8.5, for 20 min. Then, the reaction mixture was rebuffed against TBS, pH 7.6, using Zeba Spin Columns (MWCO 7,000, Pierce Biotechnology, Waltham, MA) after the addition of 10 mM EDTA. After rebuffing, a final concentration of 30 mM calcium chloride was added and the protein was purified via a mannan affinity chromatography as described earlier³.

Fluorescent Labeling of MNK and CA2

MNK was diafiltered using Amicon Ultra-15 spin filters (MWCO 10,000, EMD Millipore, Billerica, MA) against HBS buffer, pH 7.6 and afterwards concentrated to 1 mL volume. 3 mg of CA2 were dissolved in HBS buffer, pH 7.6. The protein solution was transferred into 15 mL falcon tubes. 1 mg Chromeo-642-NHS-ester dye was dissolved in 10 µL DMF. From this stock solution, in total 2 µL were added to the protein solution in 0.2 µL steps. Afterwards, the reaction was carried out for 1 h at room temperature in the dark and then quenched by adding 4 mL TBS buffer, pH 7.8 for 1 h. Excessive dye was removed by diafiltration using Amicon Ultra-15 spin filters and TBS buffer, pH 7.8 until the flow-through was colorless.

Preparation of chemical arrays

Chemical arrays were prepared using photo affinity proline linker as described previously⁴.

Optimization of the incubation conditions

To optimize the incubation conditions, we tested various methods to block the arrays (skim milk powder and BSA), to incubate the protein samples (4°C, 25°C, 1 h, overnight, with and without rotating, in presence and absence of BSA or skim milk), to detect protein binding (directly labelled, primary and secondary labelled detection) and to wash the arrays (quick and extensive). Extensive and multiple washing steps were not beneficial for signal quality, so we used directly fluorescently labelled proteins and a quick washing procedure using cold buffer (thrice for 5 s). On the other hand, this enhanced the background signal in samples with higher protein concentrations and lead to a background that was not evenly distributed in samples without mixing. A higher background signal was additionally observed when blocking the arrays with skim milk. This can probably be traced back to interactions from components of the skim milk with our lectins. In the end, using low concentrations of labelled protein after blocking the arrays with BSA while rotating during incubation

yielded the best results for Langerin and DC-SIGN (Fig. 1 A, D). The rigid proline linker outperformed the flexible PEG linker with respect to background signal and signal to noise.

Fragment immobilization

For the initial test of the array, compounds were printed in three concentrations (2.5 mM, 5 mM, and 10 mM dissolved in DMSO). For most of the compounds it was beneficial to use a higher concentration for immobilization. For Langerin 18 signals were significantly enhanced on the 10 mM spots compared to three that showed this behaviour on the 2.5 mM spots. The results for DC-SIGN were comparable (20 to three). The overall recovery rates for hits against Langerin and DC-SIGN for the 10 mM spots were 69% and 55%, respectively. Including the hits that were unique for the 2.5 mM spots, the recovery rates were 71% and 59%, respectively. Choosing higher concentrations is on average more efficient if it is not possible to optimize the immobilization concentration for each compound. This effect is probably caused by compounds with a high absorption at $\lambda = 365$ nm which is the wavelength used during the photoreaction.

Performing the micro array experiment

The arrays were blocked with 2% BSA in TBS-T (TBS with 0.05% Tween-20) for at least 1 h at room temperature while shaking. After washing thrice for 5 min with TBS-T while shaking, the protein sample was applied in a Microarray Hybridization Chamber (G2534A, Agilent Technologies, Santa Clara, CA) at 0.2 μ M. Samples were incubated overnight at 25°C in a vertical rotator. Afterwards, the arrays were washed thrice with cold TBS-T with 2 mM calcium chloride for 5 s and dried by centrifugation. Then, the arrays were scanned using a GenePix 4300A microarray scanner (Molecular Devices, Sunnyvale, CA).

Preparation of HEK293T cell lysate

A confluent 60 mm petri dish of HEK293T cells was harvested by scraping and resuspended in and washed with cold PBS (800 x g, 4°C). After another centrifugation step, the cells were resuspended in 500 μ L of sample buffer and lysed by ultrasonication (3 x 10 s).

NMR screening

The screening was performed as described previously for DC-SIGN and human Langerin¹. The same method was applied for murine Langerin as well¹. For CA2, the nanomolar inhibitor 6-Ethoxy-2-benzothiazolesulfonamide (333328, Sigma-Aldrich) was added for competition at a final concentration of 200 μ M⁵. For MNK, ATP and ManNAc were added at a final concentration of 10 mM each. Compounds that changed their signal intensity either as competitor (3%) or potential allosteric binder (5%) were considered as hits (8% in total, Aretz, *et al.*, 2016, DOI: 10.1139/cjc-2015-0603).

Data analysis of the chemical fragment arrays

Signal intensities were calculated by subtracting the mean background signals from the mean values of each spot using GenePix Pro 7 (Molecular Devices). Then, the signal data for each compound and for the DMSO spots were grouped in KNIME 2.11.0⁶ and analyzed using an ANOVA followed by Dunnett's test in GraphPad Prism 6.0 (GraphPad Software, La Jolla, CA, USA) or R 2.15.0⁷. MACCS (Molecular ACCess System) fingerprints were calculated in KNIME 2.11.0 using the MACCS Keys MOE node (Chemical Computing Group, Montreal, Canada)⁸.

Supporting figures

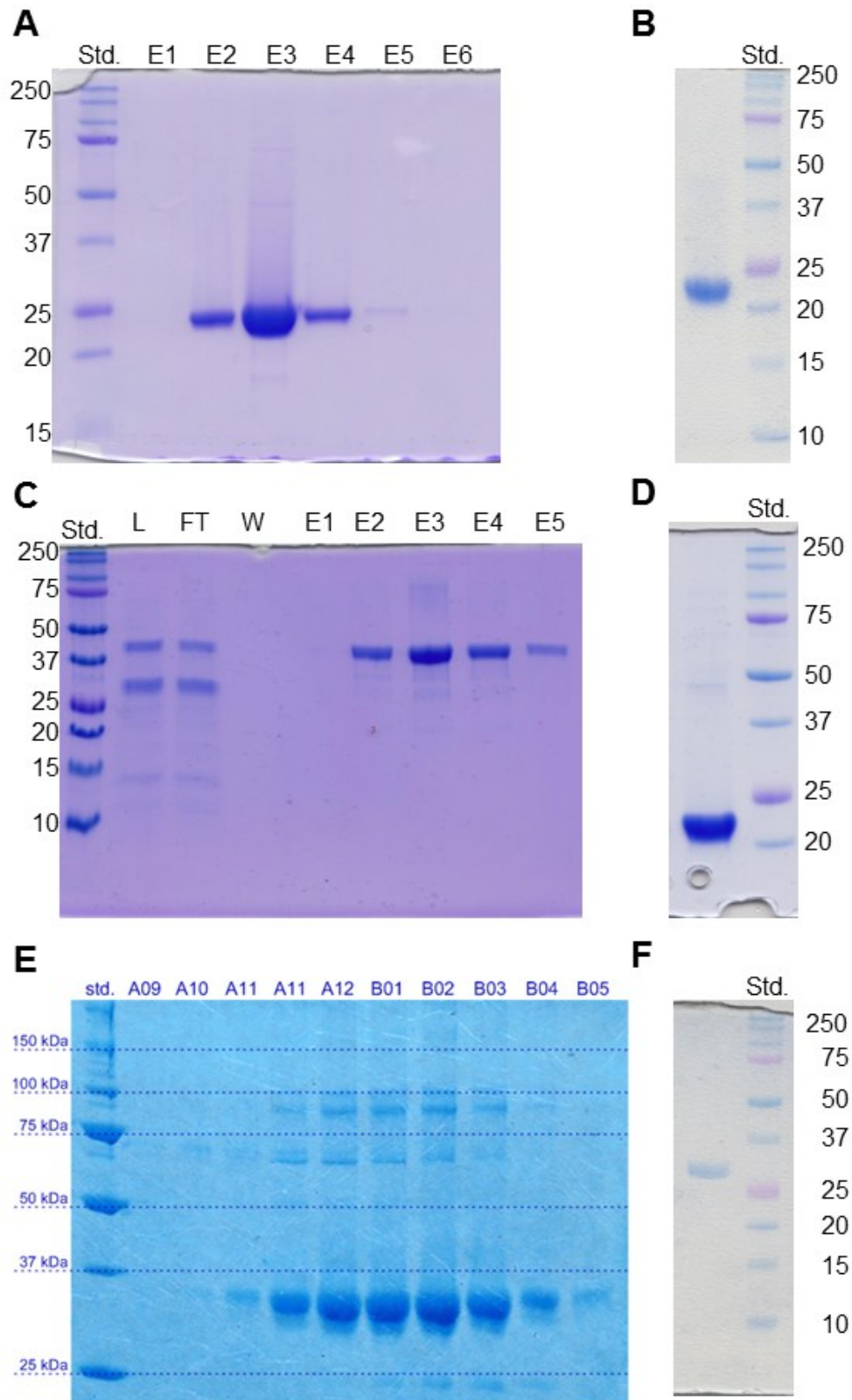


Fig. S1: Quality controls of the proteins used in this study. To monitor the purity and size of the protein preparations, SDS-PAGE was performed for murine Langerin (23 kDa, A), human Langerin (23 kDa, B), DC-SIGN extracellular domain (42 kDa, C), DC-SIGN carbohydrate recognition domain (20 kDa, D), MNK (35 kDa, E), and CA2 (30 kDa, F). Abbreviations used: Std.: standard, E: elution, L: load, FT: flow-through, W: wash.

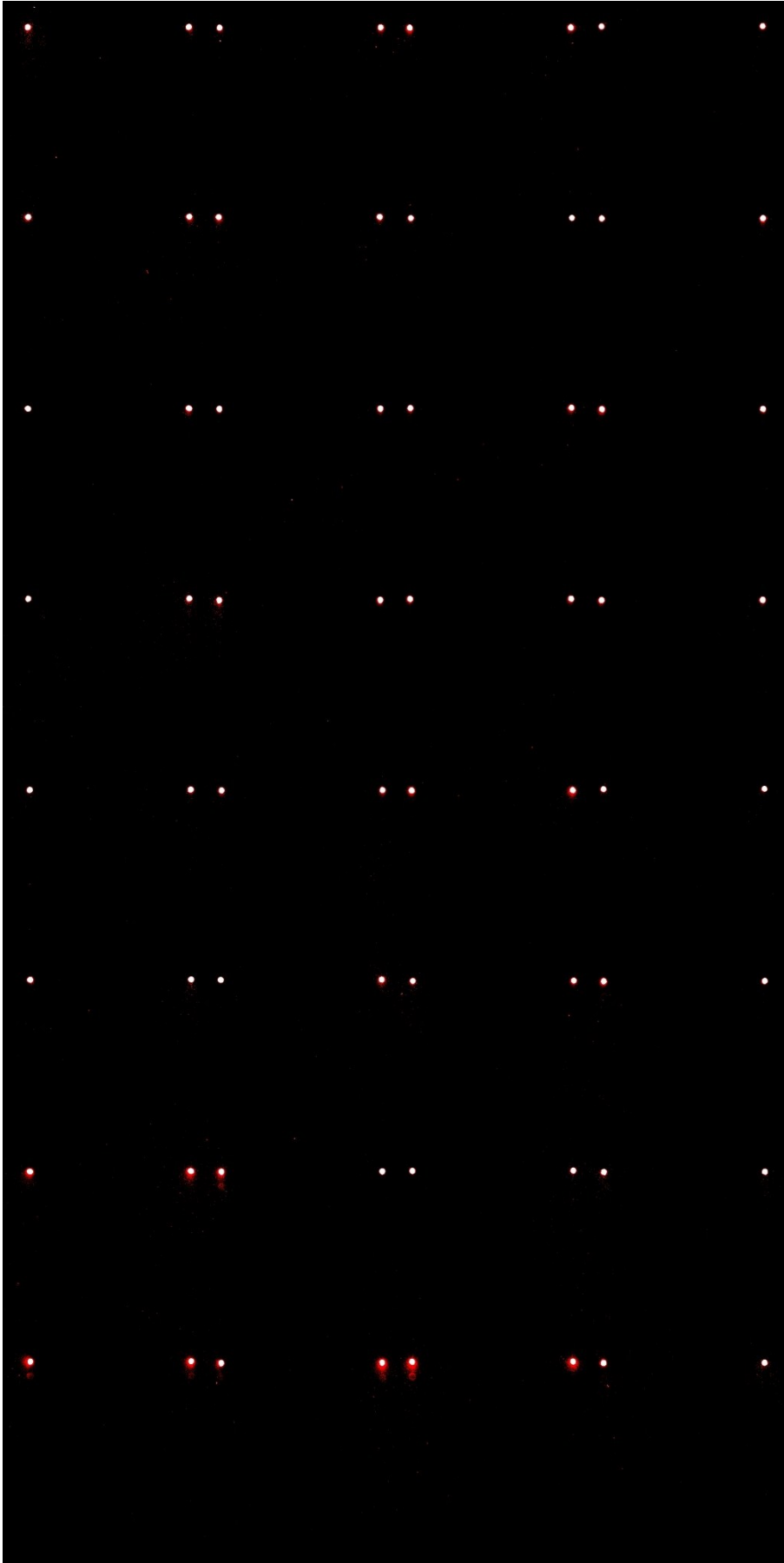


Fig. S2: Scan of an array with the highest gain to test for autofluorescence of the fragments. Only the position markers of each block gave rise to detectable signals.

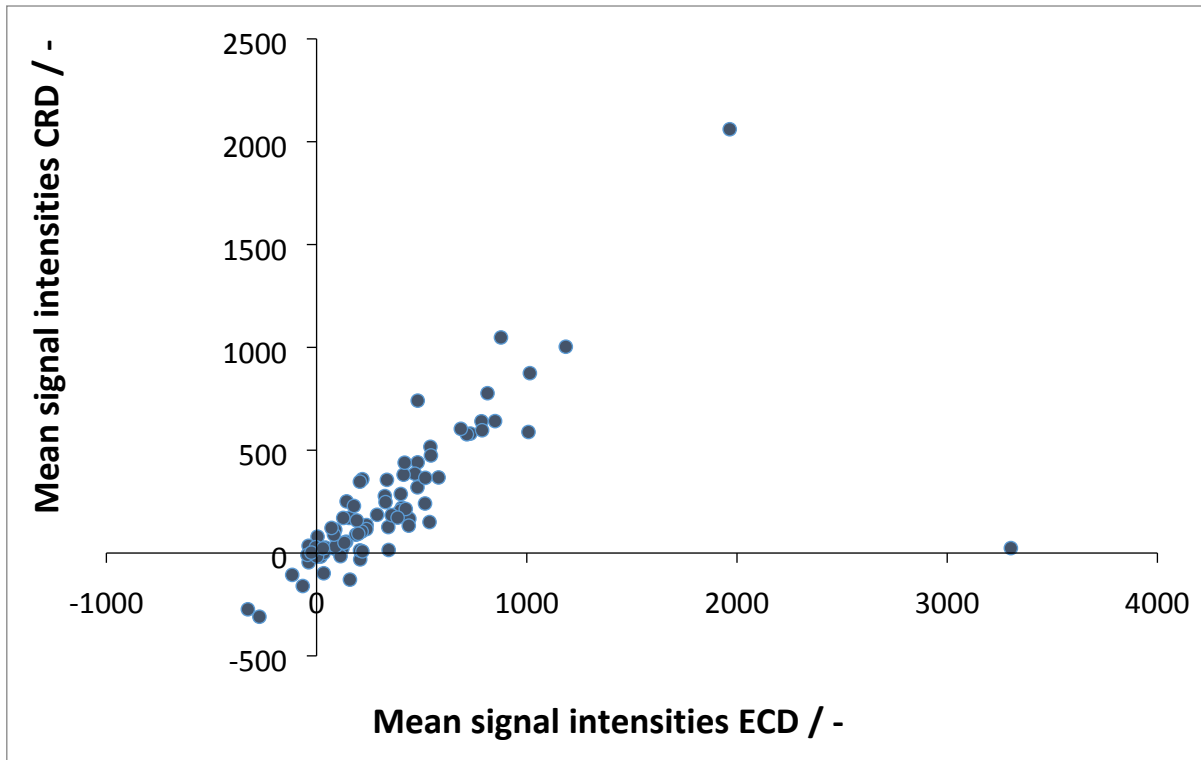


Fig. S3: Correlation of signal intensities of monomeric DC-SIGN carbohydrate recognition domain (CRD) with tetrameric DC-SIGN extracellular domain (ECD).

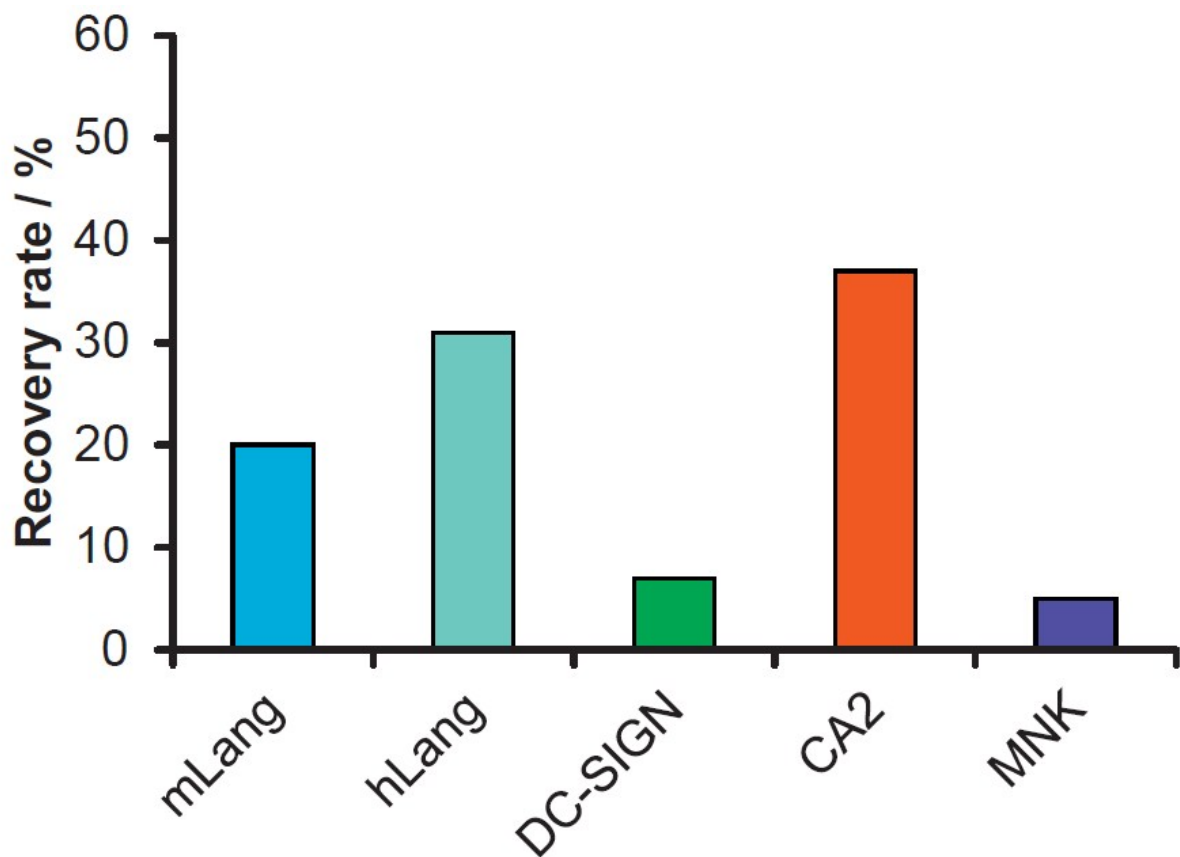


Fig. S4: Recovery rates for hits from ¹⁹F NMR screenings in array experiments using a PEG linker for fragment immobilization.

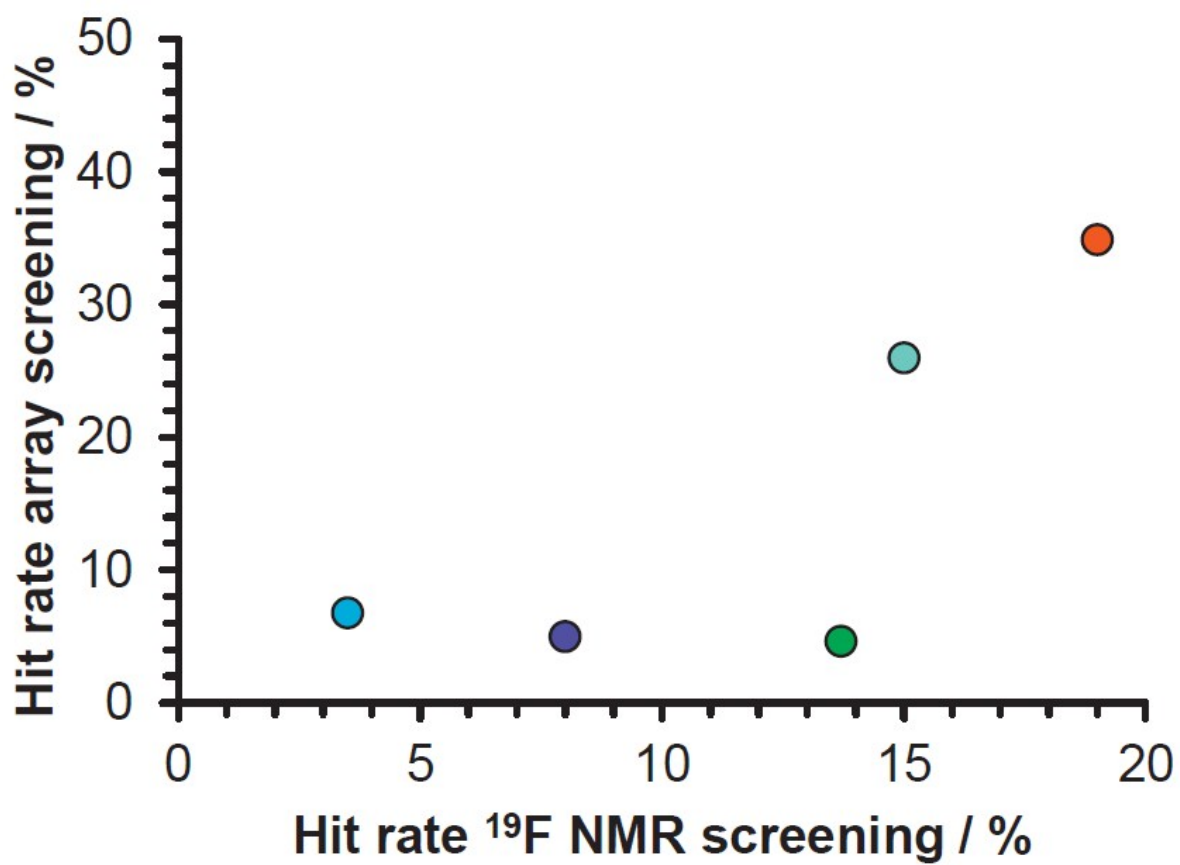


Fig. S5: Correlation of the hit rates of the array screening with the ^{19}F NMR screening using a PEG linker for immobilization.

Chemoinformatic analysis

| MACCS fingerprint | p value |
|---|---------|
| 1: #isotopes | 1,000 |
| 2: #atoms with atomic number > 103 | 1,000 |
| 3: #group IVA, VA and VIA periods 4-6 | 1,000 |
| 4: #Actinides | 1,000 |
| 5: #group IIIB, IVB elements | 1,000 |
| 6: #Lanthanides | 1,000 |
| 7: #group VB, VIB, VIIB elements | 1,000 |
| 8: #heteroatoms in 4-membered rings | 0,696 |
| 9: #group VIIIB elements | 1,000 |
| 10: #alkaline earth elements | 1,000 |
| 11: #atoms in 4 ring | 0,931 |
| 12: #group IB, IIB elements | 1,000 |
| 13: #N connected to 1 O and 2 C | 0,557 |
| 14: #S atoms in S-S groups | 1,000 |
| 15: #C connected to 3 O | 1,000 |
| 16: #heteroatoms in 3-membered rings | 1,000 |
| 17: #C in CC triple bonds | 0,747 |
| 18: #group IIIA elements | 1,000 |
| 19: #atoms in 7 ring | 0,970 |
| 20: #silicon atoms | 1,000 |
| 21: #C = bonded to C and 3 heavy atoms | 0,158 |
| 22: #atoms in 3 ring | 0,984 |
| 23: #C bonded 1 N and 2 O | 0,318 |
| 24: #O-N single bonds | 0,820 |
| 25: #C bonded to at least 3 N atoms | 0,627 |
| 26: #C in 3 ring bonds and a double bond | 0,318 |
| 27: #iodine atoms | 1,000 |
| 28: #XCH ₂ X, where X<>C | 0,568 |
| 29: #phosphorous atoms | 1,000 |
| 30: #non-C Q4 bonded to >= 3 C | 1,000 |
| 31: #halogens connected to non carbons | 1,000 |
| 32: #S bonded to an N and a C | 0,376 |
| 33: #S atoms bonded to N | 0,297 |
| 34: #CH ₂ = units | 1,000 |
| 35: #alkali (group IA) elements | 1,000 |
| 36: #S atoms in rings | 0,852 |
| 37: #C bonded to >= 1 O & >=2 N | 0,703 |
| 38: #C bonded >= 2 N and 1 C | 0,848 |
| 39: #S atoms bonded to 3 O | 0,318 |
| 40: #S single bonded to OQ ₂ | 0,318 |
| 41: #N in C#N | 0,645 |
| 42: #fluorine atoms | 0,030 |
| 43: #X-H heteroatoms 2 bonds from another | 0,008 |

| | |
|--|-------|
| 44: #other elements | 1,000 |
| 45: #N atoms adjacent to -C=C | 0,979 |
| 46: #bromine atoms | 0,419 |
| 47: #S two bonds from an N | 0,969 |
| 48: #non C bonded to >= 3 O | 0,318 |
| 49: #charged atoms | 0,195 |
| 50: #C in C=C bonded to >= 3 C | 0,196 |
| 51: #S bonded to a C and an O | 0,507 |
| 52: #N bonded to N | 0,368 |
| 53: #QH 4 bonds from another QH | 0,012 |
| 54: #QH 3 bonds from another QH | 0,000 |
| 55: #S bonded to >=2 O | 0,409 |
| 56: #N bonded to >= 2O and >= 1 C | 1,000 |
| 57: #O in rings | 0,622 |
| 58: #S bonded to >=2 non-carbon atoms | 0,409 |
| 59: #non-aromatic S-[a] | 0,984 |
| 60: #[S+]-[O-] | 0,409 |
| 61: #SQ3 | 0,409 |
| 62: #non-ring bonds that connect rings | 0,279 |
| 63: #N atoms in double bonds with O | 1,000 |
| 64: #non-ring S attached to a ring | 0,620 |
| 65: #N in aromatic bonds with C | 0,960 |
| 66: #CX4 bonded to >=3 carbons | 0,986 |
| 67: #S attached to heteroatoms | 0,454 |
| 68: #QH bonded to another QH | 0,318 |
| 69: #QH bonded to another Q | 0,814 |
| 70: #N bonded to two non-C heavy atoms | 0,920 |
| 71: #N bonded to O | 0,480 |
| 72: #O separated by 3 bonds | 0,304 |
| 73: #S in double/charge separated bonds | 0,555 |
| 74: #dimethyl substituted atoms | 0,405 |
| 75: #N non-ring bonded to a ring | 0,310 |
| 76: #C in C=C bonded to >= 3 heavy atoms | 0,654 |
| 77: #N separated by 2 bonds | 0,954 |
| 78: #N double bonded to C | 0,535 |
| 79: #N separated by 3 bonds | 0,091 |
| 80: #N separated by 4 bonds | 0,786 |
| 81: #S attached to Q >= 3 atoms | 0,854 |
| 82: #heteroatoms attached to a CH2 | 0,002 |
| 83: #heteroatoms in 5 ring | 0,616 |
| 84: #NH2 groups | 0,729 |
| 85: #N bonded to >= 3 C | 0,756 |
| 86: #CH2 or CH3 separated by non-C | 0,542 |
| 87: #halogens bonded to any ring | 0,159 |
| 88: #sulfurs | 0,869 |
| 89: #O separated by 4 bonds | 0,845 |
| 90: #het. 3 bonds from a CH2 | 0,083 |

| | |
|--|-------|
| 91: #het. 4 bonds from a CH2 | 0,038 |
| 92: #C bonded to >=1 N, >=1 C & >= 1 O | 0,212 |
| 93: #methylated heteroatoms | 0,459 |
| 94: #N bonded to non C | 0,712 |
| 95: #O 3 bonds from an N | 0,129 |
| 96: #atoms in 5-rings | 0,445 |
| 97: #O 4 bonds from an N | 0,242 |
| 98: #het. in 6-ring | 0,891 |
| 99: #C in C=C | 0,698 |
| 100: #N attached to CH2 | 0,088 |
| 101: #atoms in 8-ring or higher | 0,911 |
| 102: #O bonded to non C heavy atoms | 0,304 |
| 103: #chlorine atoms | 0,939 |
| 104: #hets. 2 bonds from a CH2 | 0,001 |
| 105: #hets. ring bonded to a 3-ring bond X | 0,939 |
| 106: #X bonded to >= 3 non-C | 0,068 |
| 107: #XQ>3 bonded to at least 1 halogen | 0,477 |
| 108: #CH3 4 bonds from a CH2 | 0,979 |
| 109: #O attached to CH2 | 0,802 |
| 110: #O 1 C from an N | 0,157 |
| 111: #N 2 bonds from a CH2 | 0,138 |
| 112: #atoms with coordination number >= 4 | 0,020 |
| 113: #O in non-aromatic bonds to an [a] | 0,514 |
| 114: #CH3 attached to CH2 | 0,355 |
| 115: #CH3 2 bonds from a CH2 | 0,752 |
| 116: #CH3 3 bonds from a CH2 | 0,586 |
| 117: #N 2 bonds from an O | 0,587 |
| 118: (key(147)-1 if key(147)>1; else 0) | 0,605 |
| 119: #N in double bonds | 0,535 |
| 120: (key(137)-1 if key(137)>1; else 0) | 0,339 |
| 121: #N in rings | 0,413 |
| 122: #N with coordination number >=3 | 0,858 |
| 123: #O separated by 1 C | 0,052 |
| 124: #het-het bonds | 0,706 |
| 125: Is # AROMATIC RING > 1? | 0,075 |
| 126: #non-ring O bonded to 2 heavy atoms | 0,704 |
| 127: (key(143)-1 if key(143)>1; else 0) | 0,622 |
| 128: #CH2s separated by 4 bonds | 0,680 |
| 129: #CH2s separated by 3 bonds | 0,212 |
| 130: (key(124)-1 if key(124)>1; else 0) | 0,690 |
| 131: (# het atoms with H) | 0,000 |
| 132: #O 2 bonds from CH2 | 0,161 |
| 133: #N non-ring bonded to a ring | 0,610 |
| 134: #halogens | 0,039 |
| 135: #N in a non-aromatic bond with [a] | 0,835 |
| 136: Bit: is there more than 1 O= | 0,567 |
| 137: Total # ring HETEROCYCLE atoms | 0,580 |

| | |
|--|-------|
| 138: (key(153)-1 if key(153)>1; else 0) | 0,191 |
| 139: #OH groups | 0,000 |
| 140: (key(164)-3 if key(164)>3; else 0) | 0,059 |
| 141: (key(160)-2 if key(160)>2; else 0) | 1,000 |
| 142: (key(161)-2 if key(161)>1; else 0) | 0,340 |
| 143: #non ring O connected to a ring | 0,425 |
| 144: #atoms separated by (!:)(!: | 0,420 |
| 145: #6M RING > 1 | 0,041 |
| 146: Key(164)-2 if key(164)>2; else 0 | 0,044 |
| 147: #CH2 attached to CH2 | 0,444 |
| 148: #non-C with coordination number >=3 | 0,839 |
| 149: (key(160)-1 if key(160)>1; else 0) | 0,713 |
| 150: #X separated by (!r)-r-(!r) | 0,675 |
| 151: #NH | 0,059 |
| 152: #C bonded to >=2 C and 1 O | 0,681 |
| 153: #non-carbons attached to CH2 | 0,141 |
| 154: #O in C=O | 0,094 |
| 155: #non-ring CH2 | 0,015 |
| 156: #XN where coord. # of X>=3 | 0,800 |
| 157: #O in C-O single bonds | 0,012 |
| 158: #N in C-N single bonds | 0,125 |
| 159: Key(164)-1 if key(164)>1; else 0 | 0,043 |
| 160: #CH3 groups | 0,245 |
| 161: #N | 0,420 |
| 162: #aromatics | 0,598 |
| 163: #atoms in 6 rings | 0,031 |
| 164: #oxygens | 0,053 |
| 165: #ring atoms | 0,002 |
| 166: Is there more than 1 fragment? | 0,116 |

Fig. S6: Difference between “non-hitters” and “regular-hitters” using MACCS fingerprints (Student’s *t*-test).

Additional discussion of chemoinformatic analysis

Notably several compounds did not show binding in any of the performed experiments even though they were identified as binders by NMR while others did in most of the cases. To explore common features we analyzed these chemoinformatically (Fig. S6). For this purpose, the 281 fluorinated fragments were separated into three groups: compounds that never showed a significantly enhanced signal in at least one experiment were considered as “non-hitters” (Dunnett’s test against DMSO controls, $p < 0.05$) while compounds that hit in at least 80% of the performed experiments were considered as “frequent hitters” (Dunnett’s test against DMSO controls, $p < 0.001$). All other compounds were considered as “regular hitters”.

“Non-hitters” were in average significantly smaller than “regular hitters” concerning MW and number of non-hydrogen atoms (21 Da and 2 HA, *t*-test, equal variances not assumed, $p < 0.001$). They also have less and smaller ring systems (#6M Ring > 1, #atoms in 6 membered rings and #ring atoms are significantly lower). Interestingly, the amount of heteroatoms in both groups was the same while the number of X-H heteroatoms was significantly lower in the “non-hitter” group (*t*-test, equal variances not assumed, $p < 0.001$). The important groups for this effect were hydroxyls but not amine groups (#OH groups significantly lower, #NH groups and #NH₂ groups not affected significantly). In a study analyzing the favored reaction products of a diazirine containing photoaffinity linker with different small organic molecules, a tendency towards a favored reaction with hydroxyl groups is observed as well⁹. This leads to the assumption that some binding epitopes are more prone to be impaired by the linker conjugation. In a larger molecule this effect is less likely as the linker has more attachment sites. Hydroxyl groups react faster with the linker and thus a reaction is more probable⁹. Thus, this group may protect other necessary binding epitopes. A higher number of hydroxyl groups per molecule may decrease the likelihood for an essential hydroxyl group to react. Alternatively, the immobilization density could be increased if fragments contain more hydroxyl groups. A feature of compounds that is known to impair the immobilization density is absorption at $\lambda = 365$ nm, the wavelength at which the photoaffinity reaction is performed. Finally, new binding epitopes may arise during the reaction of the linker, because a trifluoromethyl group and a benzamide are attached to the fragment. This effect was already observed for some compounds from the Langerin SAR that did not bind in the SPR assay but on the array.

A limited number of “frequent hitters” was observed, with only twelve fragments binding to 80% of the targets during every screening round. This low number renders a statistical analysis difficult. The only feature that was significantly enhanced in this group was the number of aromatic features (#aromatics). The higher number of aromatic substructures suggests that larger aromatic substituents may be more susceptible to false positive behavior due to non-specific binding.

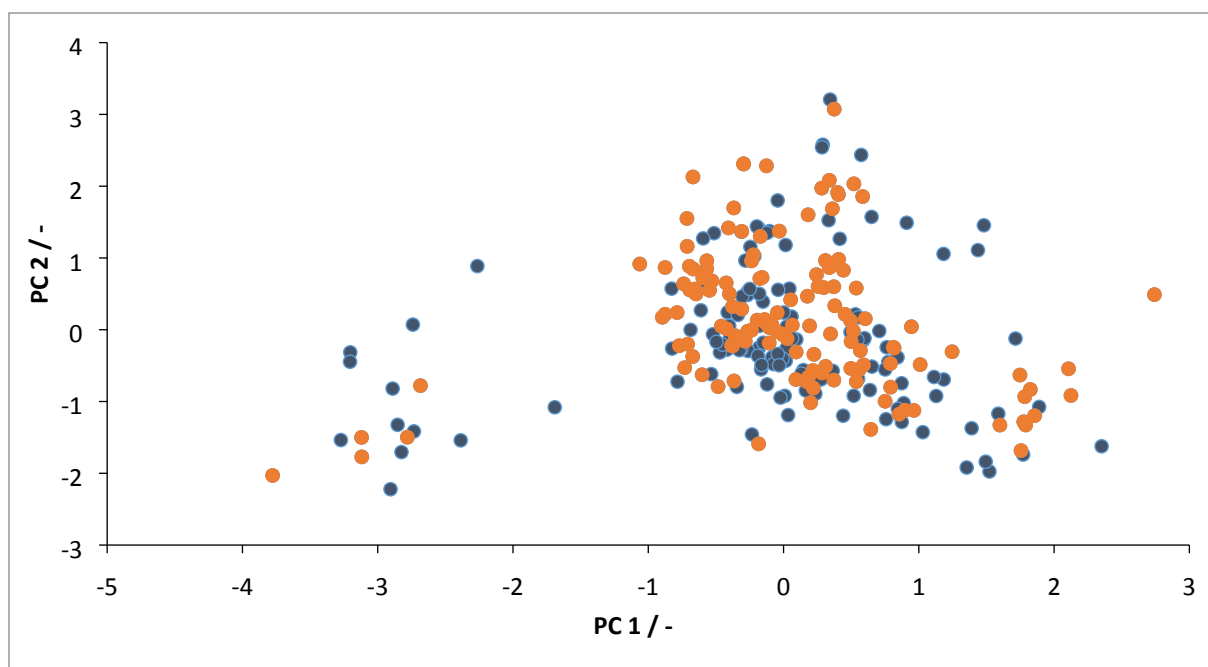


Fig. S7: Principle component analysis of MACCS fingerprints of the fragment library (blue) and the "regular hitters" data set (orange).

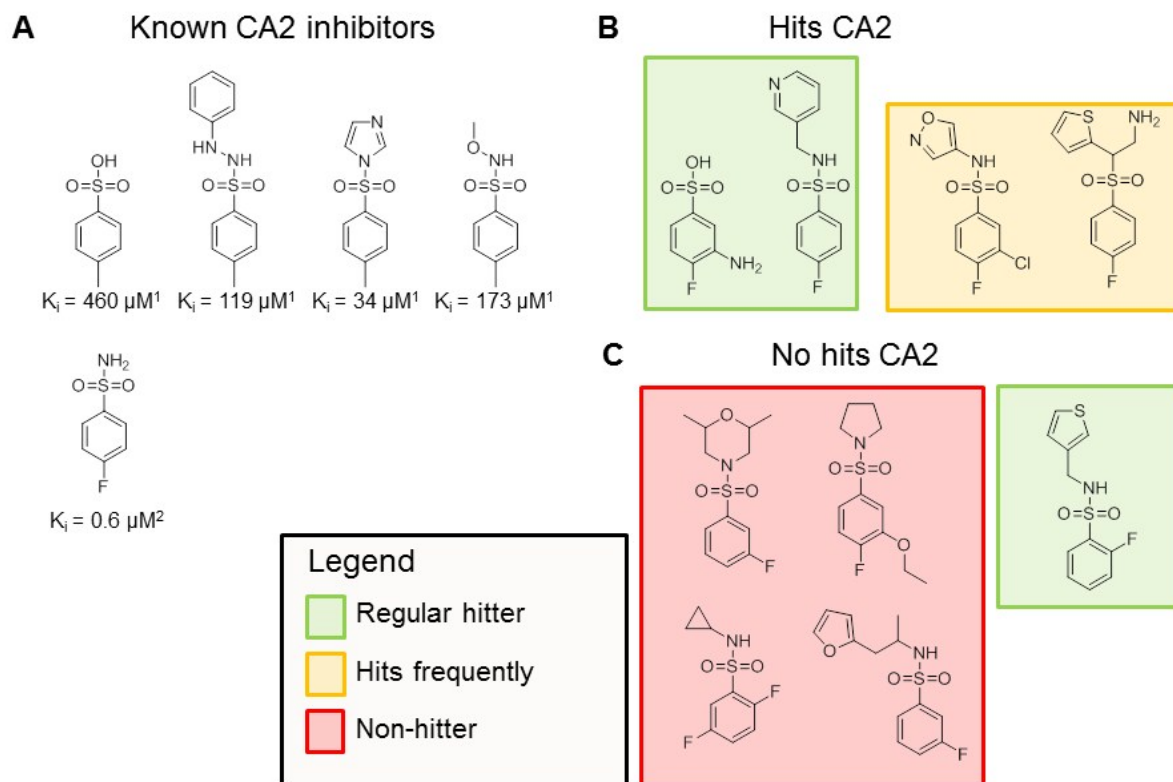


Fig. S8: Known CA2 inhibitors⁵ and related fragments present on the chemical fragment array. To analyze whether fragment arrays are able to identify suitable starting points for drug design, we found nine compounds in the immobilized library that resemble known CA2 inhibitors. (A) Previously identified inhibitors for bovine CA2^{10, 11}. (B+C) Nine fragments present on the array with high substructure similarity to known CA2 inhibitors. (B) Four were identified as hits against CA2 on the array while (C) five compounds were not identified as hits. The compounds are classified as “regular hitters” (green), “frequent hitters” (yellow) and “non-hitters” (red, see “additional discussion of chemoinformatic analysis”).

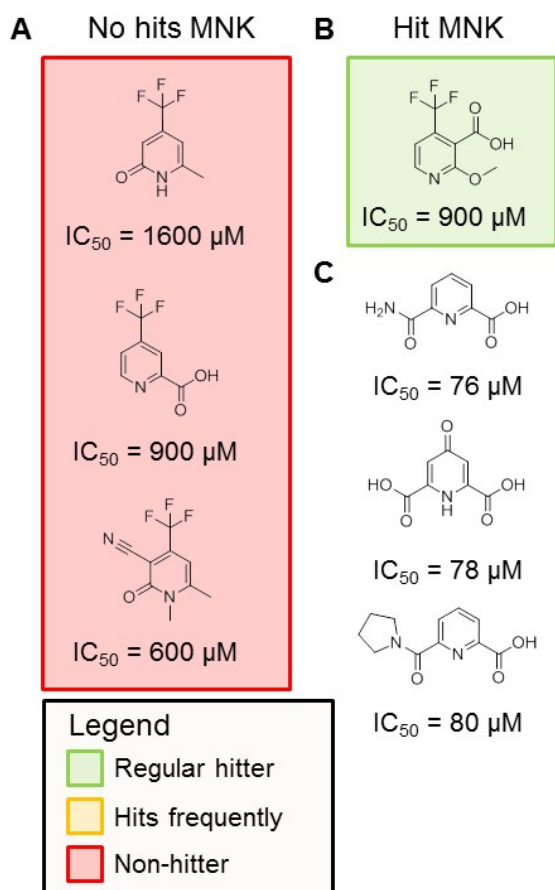


Fig. S9: MNK inhibitors from fragment-based ligand design. We previously identified picolinic acid derivatives as highly efficient fragment inhibitors against MNK (Aretz, *et al.*, 2016, DOI: 10.1139/cjc-2015-0603). Four of these inhibitors were immobilized on the fragment array. (A) Three of these four inhibitors were not identified, (B) while one fragment was a hit during the array screening. The compounds are classified as “regular hitters” (green), “frequent hitters” (yellow) and “non-hitters” (red, see “additional discussion of chemoinformatic analysis”). (C) Previously described MNK inhibitors with picolinic acid scaffold (Aretz, *et al.*, 2016, DOI: 10.1139/cjc-2015-0603).

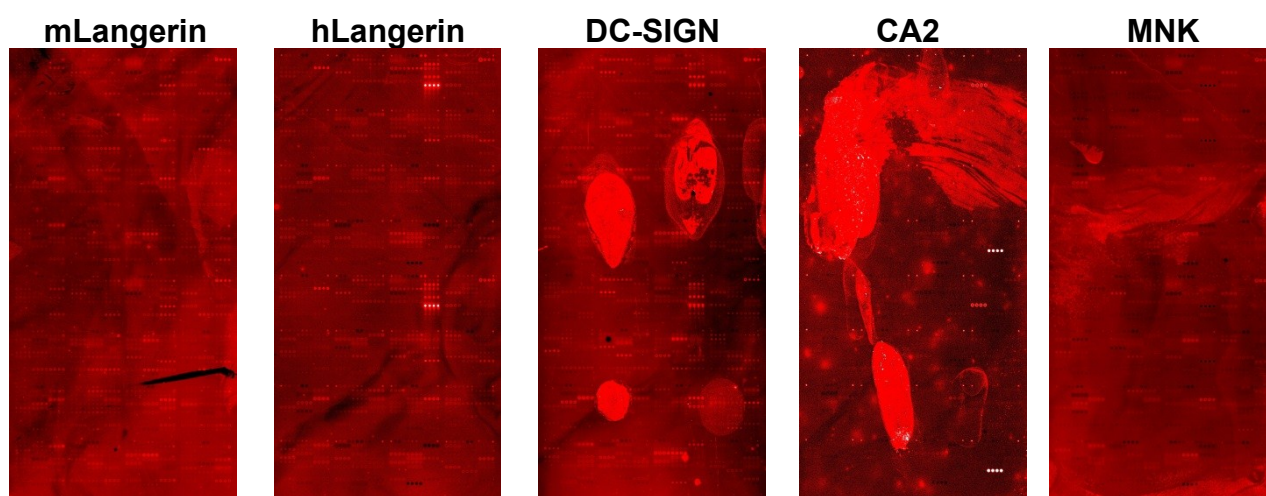


Fig. S10: Chemical arrays using $0.2 \mu\text{M}$ protein in the presence of HEK293T cell lysate.

Notes and References

1. J. Aretz, E. C. Wamhoff, J. Hanske, D. Heymann and C. Rademacher, *Frontiers in immunology*, 2014, **5**, 323.
2. J. Martinez, L. D. Nguyen, S. Hinderlich, R. Zimmer, E. Tauberger, W. Reutter, W. Saenger, H. Fan and S. Moniot, *J Biol Chem*, 2012, **287**, 13656-13665.
3. N. S. Stambach and M. E. Taylor, *Glycobiology*, 2003, **13**, 401-410.
4. Y. Kondoh, K. Honda and H. Osada, *Methods in molecular biology*, 2015, **1263**, 29-41.
5. V. M. Krishnamurthy, G. K. Kaufman, A. R. Urbach, I. Gitlin, K. L. Gudiksen, D. B. Weibel and G. M. Whitesides, *Chem Rev*, 2008, **108**, 946-1051.
6. N. C. Michael R. Berthold, Fabian Dill, Thomas R. Gabriel, Tobias Koetter, Thorsten Meinl, Peter Ohl, Christoph Sieb, Kilian Thiel, Bernd Wiswedel, in *Studies in Classification, Data Analysis, and Knowledge Organization*, Springer, 2007.
7. R Development Core Team, *Journal*, 2012, **2.15.0**.
8. I. Chemical Computing Group, *Journal*, 2013.
9. T. Suzuki, T. Okamura, T. Tomohiro, Y. Iwabuchi and N. Kanoh, *Bioconjug Chem*, 2015, **26**, 389-395.
10. F. Briganti, R. Pierattelli, A. Scozzafava and C. T. Supuran, *Eur J Med Chem*, 1996, **31**, 1001-1010.
11. V. M. Krishnamurthy, B. R. Bohall, C. Y. Kim, D. T. Moustakas, D. W. Christianson and G. M. Whitesides, *Chem Asian J*, 2007, **2**, 94-105.